ORIGINAL ARTICLE

The topside global broadcast ionospheric delay correction model for future LEO navigation augmentation

Yan Yang[1] · Fei Guo[1] · Chengpan Tang[2] · Mengjie Wu[2] · Kai Li[2] · Xiaohong Zhang[1,3] · Enyuan Tu[4]

Abstract

In this paper, we propose a solution of designing a topside broadcast ionospheric model to enable the future low earth orbit (LEO) navigation augmentation (LEO-NA) services. Considering the lack of global station observations to develop the LEO-NA ionosphere model, we utilize abundant global navigation satellite system (GNSS) data from LEO satellites to determine the topside global broadcast ionospheric delay. This delay can be combined with existing GNSS broadcast ionospheric delay correction models to determine LEO-NA ionospheric delay. First, the performance of the different-order spherical harmonic (SH) model is evaluated in generating a global topside ionospheric map. The results indicate that by increasing the order from 1 to 2, the internal and external accuracy of the model improves significantly. However, increasing the order from 2 to 8 leads to a decrease in accuracy of 0.10 and 0.11 TECU (total electron content unit) for the internal and external root mean square error. Taking into account compatibility with the Beidou global ionospheric delay correction model, limited data capacity in the navigation message, ionospheric model accuracy, and computational efficiency, we select the second-order SH model as the topside ionosphere broadcast model and outline the strategy for calculating broadcast coefficients. Finally, the accuracy of the topside global broadcast ionospheric delay correction model is evaluated during periods of high and low solar activity. The mean values of root mean square in 2009 and 2014 are 1.49 and 1.88 TECU, respectively. The model in 2009 and 2014 can correct for 67.30% and 72.49% of the ionospheric delay, respectively.

Keywords Broadcast ionospheric delay correction model · Low earth orbit (LEO) · Global topside ionosphere

1 Introduction

The ionosphere is an important part of the upper atmosphere extending from approximately 60–2000 km altitude (Schaer 1999; Kelley 2009). At this height, ions and free electrons can affect the propagation of electromagnetic waves and are associated with the frequency of signals used for ionospheric modelling (Yuan et al. 2017). Ionospheric modelling studies focus on high-precision and broadcast ionosphere delay models, respectively. High-precision and high-resolution ionosphere delay models are essential for improving the positioning accuracy of precise point positioning (PPP) (Zha et al. 2021; Zhang et al. 2022a), investigating fine structural changes in the ionosphere, and exploring the relationship between the ionosphere and natural disasters (Hernández-Pajares et al. 2011). The continuous advancement of global navigation satellite systems (GNSSs) has led to significant enhancements in the accuracy and reliability of global ionospheric models (Ren et al. 2016; Liu et al. 2020). Furthermore, the emergence of low earth orbit (LEO) constellations has provided a solution to the limitations of global ionospheric models in regions with few GNSS stations (Ge et al. 2022). Ren et al. (2020a) conducted precise ionospheric modelling using simulated GNSS and LEO navigation augmentation (LEO-NA) observations, and their results demonstrated a notable improvement in ionospheric model accuracy when combining LEO and GNSS data as opposed to using GNSS data alone. Additionally, GNSS

✉ Fei Guo
fguo@whu.edu.cn

[1] School of Geodesy and Geomatics, Wuhan University, Wuhan 430079, China

[2] Shanghai Astronomical Observatory, Chinese Academy of Sciences, Shanghai 200030, China

[3] Chinese Antarctic Center of Surveying and Mapping, Wuhan University, Wuhan 430079, China

[4] ICOE (Shanghai) Technologies Co, Ltd, Shanghai 201210, China

receivers onboard LEO satellites offer a promising opportunity to study the temporal and spatial characteristics of the topside ionosphere (Chen et al. 2017; Ren et al. 2020b).

The broadcast ionosphere delay model is commonly used for ionospheric error mitigation in single-frequency positioning (Wang et al. 2021). The ionospheric delay can be corrected by the well-known Klobuchar model with eight parameters for GPS single-frequency users (ICD-GPS-200 1983; Klobuchar 1991). For Galileo users, a 3-D electron density model (NeQuick-G) with three parameters is used to correct ionospheric delay (Angrisano 2013; Prieto-Cerdeira 2014), adapted from the NeQuick climatological model with real-time capabilities. The BeiDou Satellite Navigation System (BDS) broadcasts two types of ionospheric model coefficients on different signals. One model is based on the slightly modified Klobuchar model (CSNO 2012; Zhang et al. 2022b). The other model (Beidou global broadcast ionosphere delay correction model, BDGIM) is based on simplified spherical harmonic (SH) functions (CSNO 2018; Yuan et al 2019), which consist of nine broadcast parameters and 437 nonbroadcast coefficients. These hundreds of nonbroadcast coefficients should be stored and calculated in the GNSS chip in advance. GLONASS does not broadcast any ionospheric correction parameters. For GLONASS users, the ionospheric delay can be corrected using eight parameters of the Klobuchar model, which are broadcast by GPS. However, the receiver should include both GLONASS and GPS receiving units.

In recent decades, extensive studies on precise global and topside ionosphere models have been conducted, and broadcast ionospheric correction parameters are transmitted in the navigation messages of GPS, Galileo, and BeiDou. However, there is no study on the broadcast ionosphere model of the LEO-NA.

LEO satellites have the advantages of fast movement speed and strong signal power, which can effectively supplement and improve global positioning, navigation, and timing services of GNSS, and have received extensive attention (Li et al. 2019; Guo et al. 2023). LEO-NA, an application of a space-based radio system (Ma et al. 2022), is severely affected by the signal propagation error induced by the Earth's ionosphere. In the study of designing the LEO-NA, the ideal range of the orbital altitude is 900–1500 km (Ma et al. 2020; Deng et al. 2023). However, a recent study by Li et al. (2024), based on practical LEO navigation observations, indicates that the CENTISPACE LEO satellites are positioned at an altitude of approximately 700 km. According to Jin et al (2021), the maximum value of LEO topside ionosphere is over 12 total electron content units (TECU) at 800 km, and it is larger for CENTISPACE satellites at 700 km. Furthermore, LEE et al. (2013) demonstrate that the maximum topside vertical total electron content (VTEC) at 1336 km, as observed by JASON-1, can exceed 9 TECU

during periods of high solar activity and remains above 7 TECU during low activity. These findings show that the ionosphere delay in the LEO navigation signal has obvious difference from that in GNSS signals. For single-frequency users, the broadcast ionospheric model is the main method for mitigating ionospheric delay and enhancing real-time service accuracy. Wang et al. (2021) analyze the different GNSS broadcast ionospheric model performance. The RMS of BDGIM compared to Jason-2/3 reference VTECs can achieve 9 TECU, and the performance of BDGIM is the best among GNSS broadcast ionospheric delay correction model. It means the ionospheric delay can achieve about 1 m using BDGIM in LEO-NA at 1300 km when the LEO frequency is consistent with BDS. For the LEO-NA with orbital altitudes below 1300 km, the performance of GNSS broadcast ionospheric models is relatively poorer. Therefore, it is crucial to establish the broadcast ionospheric model for LEO-NA.

However, there are two major difficulties in LEO-NA broadcast ionospheric modelling. First, few monitoring stations provide LEO observations, as the LEO-NA constellation is still in the design and construction stage. Second, the mathematical structure of the LEO-NA broadcast ionospheric model needs to strike a balance between simplicity and accuracy. The mathematical structure not only affects its ability to describe and model the global ionospheric total electron content (TEC) but also determines the number of coefficients required for implementation and their impact on communication capacity (Abhigna et al. 2021). Achieving high-precision ionospheric delay correction often necessitates a relatively complex mathematical structure for the model. However, the limited number of coefficients available needed a simpler structure to meet communication capacity requirements. These two factors are interdependent, and it is crucial to effectively overcome this technological bottleneck in modelling.

In this paper, we propose a solution to establish a global LEO topside broadcast ionospheric delay correction model, and the ionospheric delay LEO-NA can be determined by this model and existing GNSS broadcast ionospheric delay correction models. There are many scientific experiment satellites equipped with dual-frequency GPS receivers for precise orbit determination, which provides a promising opportunity to verify our solution.

The structure of this paper is as follows: Sect. 2 presents the methodology of the topside ionospheric delay correction model in detail. Data collection, experimental schemes, and validation methods are described in Sect. 3. Then, Sect. 4 shows the solution of topside broadcast ionospheric delay correction model and its performance at different solar activity. Finally, conclusions are provided in the last section.

2 Data and method

With the development of LEO-NA constellations, there will be abundant ground-based stations, and the LEO TEC observables will be used to establish a global LEO-NA broadcast ionosphere delay correction model. As the navigation signal of the LEO is affected by the bottom ionosphere, the LEO-NA broadcast ionospheric delay can also be obtained as follows:

$$I_{\text{LEO - NA}} = I_{\text{GNSS}} - I_{\text{topside}} \tag{1}$$

where $I_{\text{LEO - NA}}$ and I_{GNSS} denote the LEO-NA and GNSS broadcast ionosphere ionospheric delay correction, respectively, and I_{topside} denotes the broadcast ionospheric delay correction from LEO satellites to GNSS satellites. As the GNSS broadcast ionosphere ionospheric delay correction is stable and mature, the focus of this study is to construct a topside broadcast ionospheric model and evaluate its accuracy. SH can provide a precise representation of the global ionosphere TEC, and BDGIM is also developed based on the SH. The SH coefficients used in topside ionosphere modelling are analysed to strike a balance between achieving high-precision global ionospheric TEC estimation and minimizing the number of broadcast coefficients.

2.1 Observational data

Considering practical LEO-NA constellation and the study of designing the LEO-NA constellation, the COSMIC and MetOp-A have similar altitudes of 800 km in the range of LEO-NA orbital altitude. Moreover, those satellites can provide abundant observation to establish topside ionosphere model. Table 1 shows the basic information of the 7 LEO satellites selected to conduct this research, including the orbital altitude, orbit type, orbital inclination, and launch time. The COSMIC mission is a program designed to provide advances in meteorology, ionospheric research, climatology, and space weather, and its constellation includes six microsatellites. It was launched in mid-April 2006, and retired in 2020, and satellites gradually dispersed to their final orbits at ~ 800 km during the first 17 months after the satellites were launched. The MetOp-A is designed to deliver continued, long-term datasets to support operational meteorology, environmental forecasting, and global climate monitoring. This mission has an altitude of 817 km and an inclination angle of 98.7°. Chen et al (2017) show that the precision and reliability of the model created by the COSMIC and MetOp-A are better than those using the COSMIC data alone. Figure 1 shows the global distribution of topside ionospheric pierce points (TIPPs) within 4 h. The increasing number of LEOs yields a greater abundance of observational data, while simultaneously ensuring a more equitable global distribution of TIPPs.

This research utilized the PodTec products from the COSMIC and MetOp-A satellites, which were obtained from the COSMIC Data Analysis and Archive Center (CDAAC), to calculate TEC. The PodTec files provide UTC, three-dimensional coordinates of LEO and GPS satellites, observation elevation of the GPS-LEO observation link at the LEO satellite and the slant TEC (STEC) on a signal path which's accuracy levels the phase to the pseudorange. Notably, while the COSMIC PodTec product has undergone corrections for the differential code bias (DCB) of satellites and receivers, the DCB of MetOp-A has not been corrected in the product (Chen et al. 2017).

2.2 Global topside ionosphere modelling

Considering the orbital altitude of LEO satellites, the topside ionospheric electron content can be assumed to be a thin shell, as illustrated in Fig. 2. PodTec products can provide the STEC along a signal propagation path, and can be converted to VTEC using the following formula:

$$\text{STEC} = M(z) \times \text{VTEC} + \text{DCB}_r \tag{2}$$

where the mapping function $M(z)$ depends on the zenith of angle z of the slant ray path. Zhong et al. (2016) examined the application of three mapping functions for LEO-based GNSS observations and illustrated that the F&K geometric mapping function is best suited for LEO-based TEC conversion. Therefore, the F&K mapping function (Foelsche & Kirchengast 2002) is employed for LEO topside TEC conversion, converting topside STEC to topside VTEC at each TIPP. The F&K mapping function can be expressed via the following formula:

$$M(z) = \frac{1 + R_{pp}/R_{orb}}{\cos z + \sqrt{\left(R_{pp}/R_{orb}\right)^2 - (\sin z)^2}} \tag{3}$$

where $R_{pp} = R_e + H_{pp}$, $R_{orb} = R_e + H_{orb}$, R_e is Earth's radius, H_{pp} is defined as the altitude of the TIPP, and H_{orb} is the orbit altitude of LEO satellites.

It is feasible to fit the STEC using the SH model to produce a LEO topside global ionosphere model. The SH are defined as follows:

$$
\begin{aligned}
&\text{VTEC}\,(\beta,\, s,\, t) \\
&= \sum_{n=0}^{N} \sum_{m=0}^{n} \tilde{P}_{nm}\,(\sin \beta)\,\left(\tilde{c}_{n,m,t} \cos\,(ms) + \tilde{s}_{n,m,t} \sin\,(ms)\right)
\end{aligned}
\tag{4}
$$

where β and s are the latitude and sun fixed longitude of the pierce point, respectively; $\tilde{P}_{nm}$ are normalized associated

Table 1 Information on LEO satellites used in this analysis

Satellite	Altitude (KM)	Orbit type	Inclination (°)	Launch
COSMIC-1	800	Drifting	72	2006/04/14
COSMIC-2	800	Drifting	72	2006/04/14
COSMIC-3	800	Drifting	72	2006/04/14
COSMIC-4	800	Drifting	72	2006/04/14
COSMIC-5	800	Drifting	72	2006/04/14
COSMIC-6	800	Drifting	72	2006/04/14
MetOp-A	827	Sun-synchronous	98.7	2006/10/19
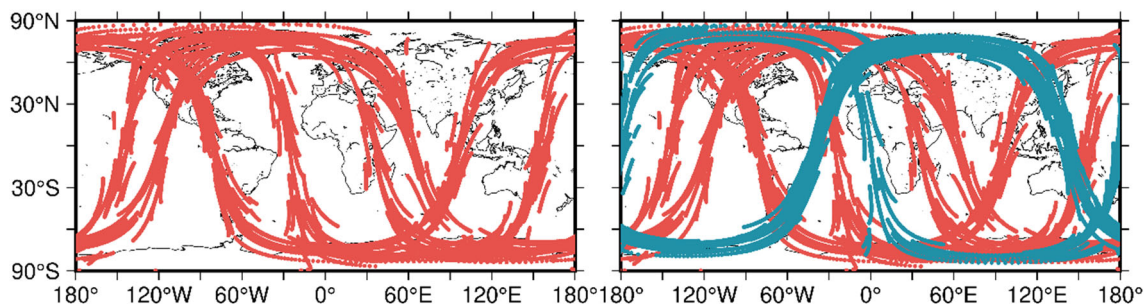
Fig. 1 Global TIPPs of COSMIC and MetOp-A satellites with 4 h. (left) Only COSMIC constellations; (right) COSMIC and MetOp-A

Legendre functions with degree n and order m; $\tilde{c}_{n,m,t}$ and $\tilde{s}_{n,m,t}$ are coefficients of SH to be determined at time t; and N is the maximum degree of the SH.

The topside TEC derived from PodTec and the variation in the topside ionosphere at time t can be calculated and described by Eq. (4). However, the number of topside ionospheric observations is limited, which may lead to data gaps. Thus, the coefficients of SH are estimated every several hours on a global scale. According to Eqs. (2–4), assuming that there are q GPS satellites tracked by COSMIC and MetOp-A satellites in a given epoch, the observation equation can be formed as follows:

$$
\begin{pmatrix} \text{STEC}_C^1(t) \\ \vdots \\ \text{STEC}_C^q(t) \\ \text{STEC}_M^1(t) \\ \vdots \\ \text{STEC}_M^q(t) \end{pmatrix} = \begin{pmatrix} M(z_C^1(t)) & \cdots & 0 & 0 & \cdots & 0 & 0 \\ \vdots & \vdots & \vdots & \vdots & \vdots & \vdots & \vdots \\ 0 & \cdots & M(z_C^q(t)) & 0 & \cdots & 0 & 0 \\ 0 & \cdots & 0 & M(z_M^1(t)) & \cdots & 0 & 1 \\ \vdots & \vdots & \vdots & \vdots & \vdots & \vdots & \vdots \\ 0 & \cdots & 0 & 0 & \cdots & M(z_M^q(t)) & 1 \end{pmatrix}
$$

$$
\times \begin{pmatrix} \text{VTEC}_C^1(\beta, s, t) \\ \vdots \\ \text{VTEC}_C^q(\beta, s, t) \\ \text{VTEC}_M^1(\beta, s, t) \\ \vdots \\ \text{VTEC}_M^q(\beta, s, t) \\ \text{DCB}_M \end{pmatrix} \qquad (5)
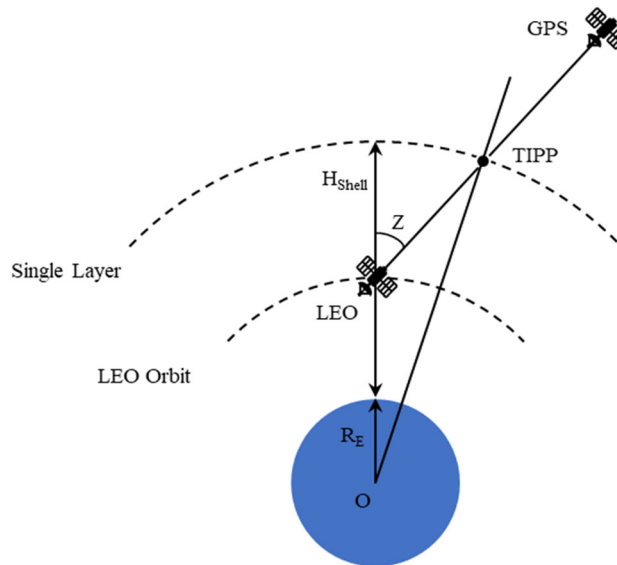$$

Fig. 2 Single-layer model of the LEO topside ionosphere

where C and M respectively mean COSMIC and MetOp satellites; DCB_M is the MetOp-A GPS receiver DCB value.

3 Processing strategy and assessment method

To comprehensively demonstrate the statistical results, the performances of the topside TEC are evaluated from day
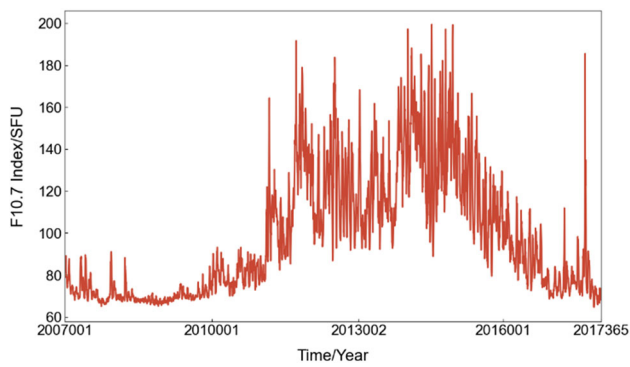
Fig. 3 Solar conditions from 2007 to 2017

Table 2 Detailed modelling strategies used in this study

Items	Processing strategy
Sampling rate	10 s
Height of thin layer	1200 km
Fitting function	Spherical harmonics expansion with the different degree and order
Estimated parameters	Spherical harmonics coefficients and MetOp-A DCB
Estimator	Least square method
Time spacing for map	4 h
Mapping Function	F&K mapping function
Reference Frame	Sun-fixed geomagnetic coordinate
Cut-off elevation	15°

of year (DOY) 001, 2009 to DOY 365, 2009, and DOY 001, 2014 to DOY 365, 2014. The solar conditions from are shown in Fig. 3. The experimental period covers nearly one solar cycle. Given that the sampling rate of the original data is 1 s, the amount of data is large, and the sampling rate is reduced to 10 s. Based on the thin layer assumption, the shell height of the plasmasphere is set to 1200 km (with an ionospheric range from 800 km to 20,200 km). Considering that the topside TEC is small and the structure of the plasmasphere is less complex than that of the whole ionosphere, a spherical harmonic function with 9 × 9 or 8 × 8 order (Chen et al. 2017) has been adopted in some related studies to establish a global plasmasphere model. In this study, the max order is set to 8 and different order models are used to analyze the performance of ionospheric delay correction. The F&K mapping function is employed for topside ionospheric observation conversion. The total number of sessions is 6, ensuring the sufficient observations to achieve global modelling. The least-squares method is employed to estimate the spherical harmonic coefficients and MetOp-A DCB. The cut-off elevation was set as 15°. The detailed modelling strategies are listed in Table 2.

The root mean square error (RMSE) is chosen as the criterion to evaluate the internal and external precision of the model. The expression is as follows:

$$\text{RMSE} = \sqrt{\frac{1}{N}\sum_{i=1}^{N}\left(\text{STEC}_{model,i} - \text{STEC}_{ref,i}\right)^2} \quad (6)$$

where $\text{STEC}_{model,i}$ is the calculated STEC from the SH model and mapping function; N is the total number of values. In the calculation of the internal RMSE, the PodTec used to fit the model is regarded as $\text{STEC}_{ref,i}$. When calculating the external RMSE, the $\text{STEC}_{ref,i}$ is from the PodTec that is not used during the model's establishing. The commonly used evaluation indicators for the accuracy of ionospheric time delay model correction include the mean bias, root mean square (RMS), and correction percentage (PER) between the calculated TEC values of different ionospheric models and the ionospheric TEC reference values (Yuan et al. 2019). Bias and RMS represent the average value and root mean square, respectively, of the difference between the ionospheric TEC calculated based on the ionospheric delay correction model and the reference ionospheric TEC. PER represents the percentage of correction by the ionospheric delay correction model relative to the reference ionospheric TEC. Bias and RMS are absolute accuracy indicators, while PER is a relative accuracy indicator. The three evaluation indicators are expressed as follows:

$$\text{Bias} = \sum_{i=1}^{N} \frac{\text{TEC}_{model}^i - \text{TEC}_{ref}^i}{N} \quad (7)$$

$$\text{RMS} = \sqrt{\frac{\sum_{i=1}^{N}\left(\text{TEC}_{model}^i - \text{TEC}_{ref}^i\right)^2}{N}} \quad (8)$$

$$\text{PER} = \left(1 - \frac{1}{N}\sum_{i=1}^{N}\frac{abs\left(\text{TEC}_{model}^i - \text{TEC}_{ref}^i\right)}{\text{TEC}_{ref}^i}\right) \times 100\% \quad (9)$$

where TEC_{model}^i is the calculated TEC from the model; TEC_{ref}^i is the reference TEC; and N is the total number of values.

4 Solution and results

To obtain a high-precision and high-resolution global topside ionospheric map (GTIM), the SH function with 9 × 9 or 8 × 8 is commonly used in the modelling process. The maximum order is set as 8 in this paper. First, this
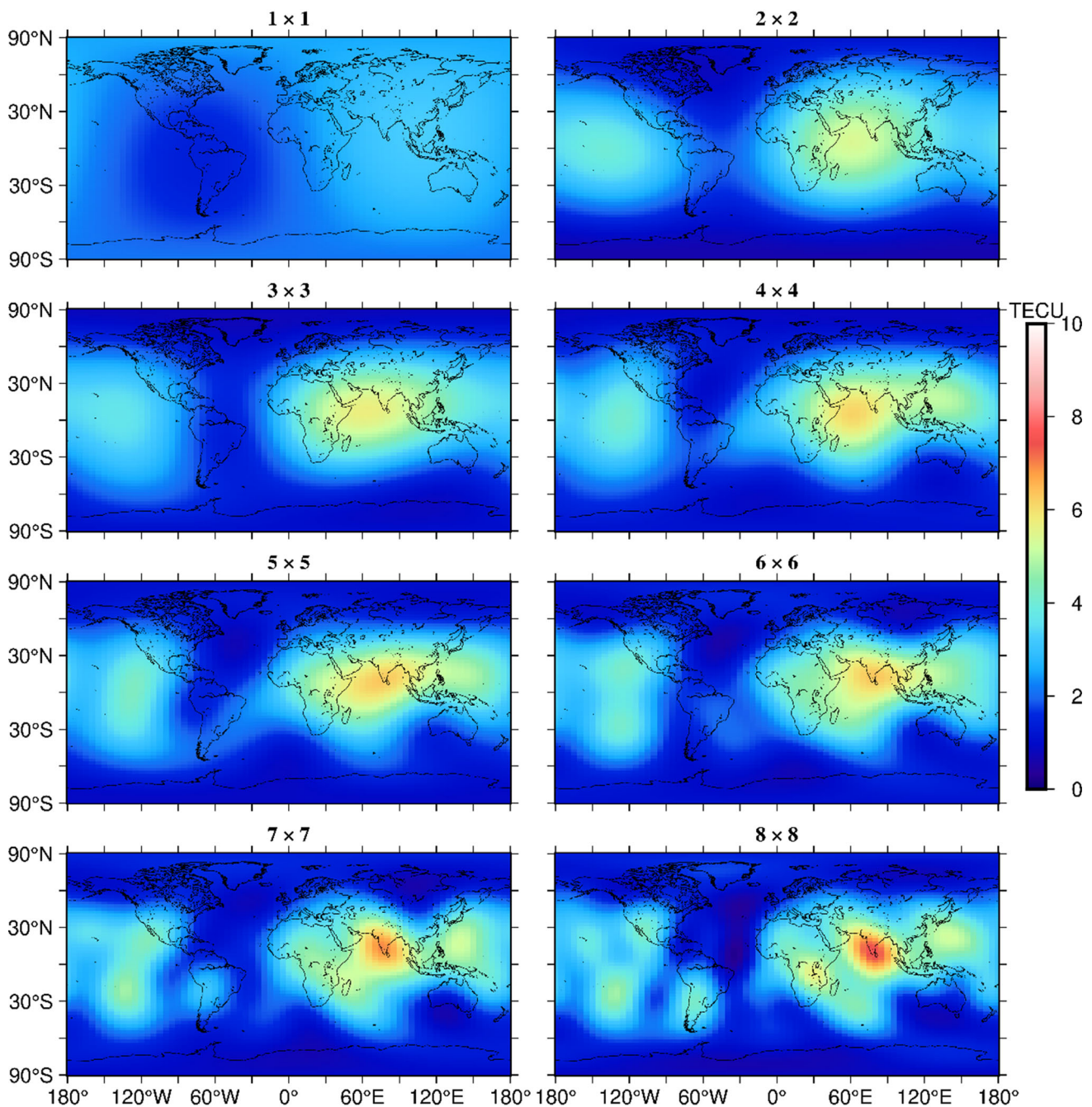
Fig. 4 Performance of the GTIMs with different orders at 10:00:00 UT, DOY 206, 2009

section evaluates the effectiveness of SH models with different orders. Then, the topside ionosphere broadcast model coefficients are determined. Finally, the topside ionospheric delay correction effect is analysed during periods of high and low solar activity.

4.1 Performance of different order topside ionosphere model

The order of the SH function represents the global resolution of the physical parameters it describes, and the corresponding coefficients of each component have certain physical meanings. The distribution of the topside global ionospheric VTEC at 10:00:00 UT on DOY 206 2009, obtained from the topside global spherical harmonic function ionospheric TEC
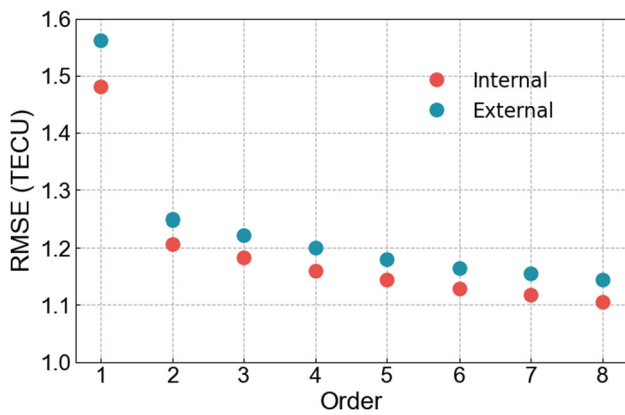
Fig. 5 The internal and external RMSEs of SH models with different orders

Table 3 The RMS and PER for SH models with different orders

Order	RMS (TECU)	PER (%)
1	0.99	64.32
2	0.54	78.51
3	0.47	81.86
4	0.46	83.46
5	0.41	84.55
6	0.37	86.63
7	0.34	88.85

model of different orders, is given in Fig. 4. The horizontal coordinates denote geographic longitude, and the vertical coordinates indicate geographic latitude. The order of the corresponding spherical harmonic function is labelled on the upper side of each plot. As the order of the spherical harmonic function increases, the resolution of the global ionospheric TEC gradually increases. However, as the order of spherical harmonics increases, the number of estimated parameters in the functions also increases. Due to the limited number of TIPPs and their uneven global distribution, the model may yield negative values for VTEC when computed globally. The difference in the topside VTEC values for different orders of SH is not significant because there is a small electron content in the topside ionosphere.

Figure 5 shows the internal and external precision of different order spherical harmonic functions. As the order of the model increases, the internal and external accuracy improves. Specifically, when the order is increased from 1 to 2, the internal and external accuracy of the model improves significantly. The internal and external RMSE decrease from 1.48 and 1.56 TECU to 1.21 and 1.25 TECU, respectively. In addition, as the order continues to increase from 2, the improvement in accuracy is relatively small. The increase in order from 2 to 8 results in a decrease in accuracy of 0.10 and 0.11 TECU for the internal and external RMSE.

The values from 8th order spherical harmonic functions are regarded as the reference ionosphere VTEC, and Table 3 shows the RMS and PER for SH models of different orders. The first-order model, which has 0.99 TECU and corrects only for 64.32% of the ionospheric delay, has the worst performance. When the order increases to 2, the performance of the model is significantly improved. The value of RMS decreases to 0.54 TECU and the correction percentage increases to 78.51%. As the order continues to increase, the improvement in model performance becomes more gradual, and the values of RMS and correction percentage are 0.34 TECU and 88.85% with the 7th order model.
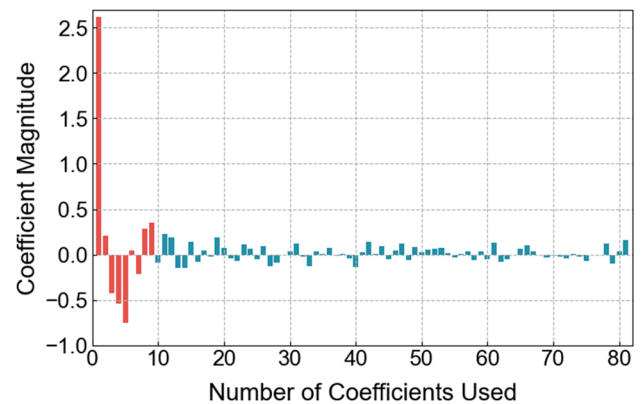

Fig. 6 All 81 coefficients of the eighth-order SH model (The first 9 coefficients and the remaining 72 coefficients are represented using different colours)

4.2 Determination of the topside ionosphere broadcast model

The SH function is a solution of the Laplace equation in spherical coordinate form. Coefficients of different orders represent the amplitudes of signals of different frequencies and the contribution of signals of different frequencies to the composite signal. Increasing the number of broadcasting coefficients can enhance the accuracy of ionosphere broadcasting. Since significantly less data capacity is desirable for communication, the number of broadcast coefficients for ionospheric model is limited (Abhigna et al. 2021). From the exiting GNSS broadcast ionospheric models, the numbers of broadcast coefficients in GPS Klobuchar, NeQuick-G, and BDGIM respectively are 8, 3, and 9. Figure 6 shows the coefficients of the 8th order SH function model. It is evident from the figure that the maximum information carried by all 81 coefficients is truncated to the first 9 coefficients, and the remaining 72 coefficients have lower magnitude. The simple truncation of the number of spherical harmonics function model coefficients from 81 to 9 is selected as a trade-off between navigation data handling capability and the accuracy of the ionospheric model. The maximum magnitudes
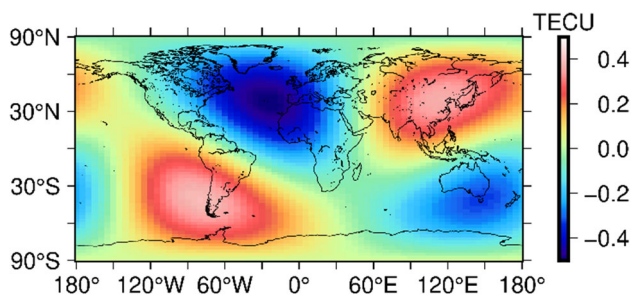
Fig. 7 Difference between the GTIM obtained using the initial 9 coefficients of the 8th order SH model and the GTIM obtained using the 2nd order SH model on DOY 206, 2009
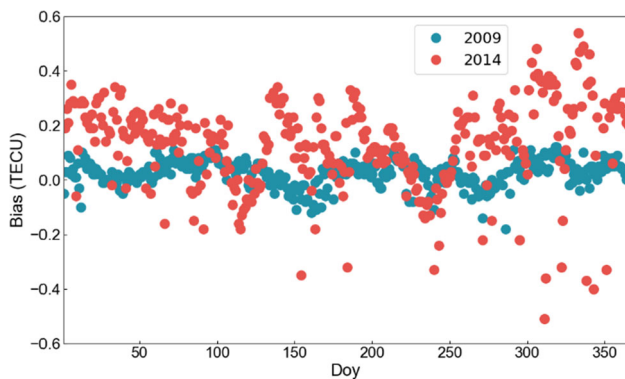

Fig. 8 The daily bias between the GTIM obtained using the initial 9 coefficients of the 8th order SH model and the GTIM obtained using the 2nd order SH model in 2009 and 2014

of spherical harmonics function coefficient information are retained in the first 9 coefficients of the eighth-order model; only those coefficients are broadcast to the users to estimate the topside ionospheric delay error.

However, it is noteworthy that the number of 2nd order SH model coefficients is also 9, and the difference between 2nd order and 8th order SH model is not significant. The differences between the GTIM obtained from the initial 9 coefficients of the 8th order SH model and the GTIM using the 2nd order SH model are depicted in Fig. 7. The max value is less than 0.5 TECU. To comprehensively evaluate the bias between the two GTIMs, the daily average bias in 2009 and 2014 is computed and shown in Fig. 8. Compared to the LEO topside ionosphere, the difference can be ignored. Considering the computational efficiency of modelling, it is more appropriate to select the coefficients of the 2nd order SH function model as the LEO-NA topside broadcast ionospheric model coefficients.

From Eq. (1), the LEO-NA ionospheric delay is computed by the GNSS and LEO-NA topside broadcast ionospheric delay corrections. The BDGIM is also based on the SH model, and the strategy of LEO-NA topside ionospheric model is consistent with the BDGIM. The BDGIM coefficients are updated every 2 h, and the previous 24 h of

actual GNSS measurements are used for solving the ionospheric model parameters in each calculation. Similarly, the 9 broadcast parameters of the LEO-NA topside broadcast ionospheric model are updated every 2 h, and a similar processing strategy shown in Fig. 9 is adopted for its parameter solving (Wang 2017). This can avoid the failure of model parameter solving due to the lack of observational data in the corresponding time period.

4.3 Performance of the topside ionosphere broadcast model

To present a comprehensive comparison, the quality of the topside global broadcast ionospheric delay correction model is accessed in 2009 and 2014. Due to the lack of high-precision external reference GTIM values, PodTec in effective range time is chosen to evaluate the RMS and PER of the topside broadcast ionospheric model. Figure 10 shows the daily RMS values in 2009 and 2014. The blue points represent 2009, and the red points represent 2014. The mean RMS values in 2009 and 2014 are 1.49 TECU and 1.88 TECU. Overall, the RMS of 2014 is slightly higher than that of 2009. Figure 11 shows the daily PER values of the topside broadcast model in 2009 and 2014. The mean values of PER in 2009 and 2014 are 67.30% and 72.49%, respectively. Compared with the results in 2009, the PER values are larger in 2014. Overall, the values of PER and RMS are more stable in 2009. Notably, 2014 is the most active year within the solar activity cycle, and the value of the LEO topside ionosphere is the largest at this time. The PER reflects the relative accuracy improvement of the model, while the RMS reflects the absolute accuracy. When the TEC reference value is large, even if the relative accuracy indicator is high, the absolute error value may still be large. Generally, in years with high ionospheric activity, the relative accuracy indicator is higher, while the absolute accuracy indicator tends to be lower.

Figure 12 shows the performance of topside broadcast ionospheric model at different local time (LT) in 2009 and 2014. The variation of yearly average LEO topside TEC with LT is shown in Fig. 12a. The variation in 2009 and 2014 shows the same tendency. The mean electron content reaches its daily maximum at LT 14:00, and it is respectively 3.89 and 6.03 TECU in 2009 and 2014. The daily minimum is at LT 4:00, and it is respectively 3.02 and 4.81 TECU. Figure 12b shows the variation of yearly RMS with LT. In 2009, the RMS value increases during LT 0:00–3:00, 5:00–9:00, and 12:00–18:00. It reaches the daily maximum value, 1.57 TECU, at LT 18:00, and the daily minimum value, 1.43 TECU, at LT 5:00. In 2014, the RMS value increases during LT 0:00–2:00, 4:00–14:00, and 17:00–18:00. It reaches the maximum value, 2.03 TECU, at 14:00, and the minimum value, 1.69 TECU at 23:00. Figure 12c shows the LT variation in the yearly PER of the LEO topside global broadcast

Fig. 9 The strategy of updating LEO-NA topside broadcast ionospheric parameters
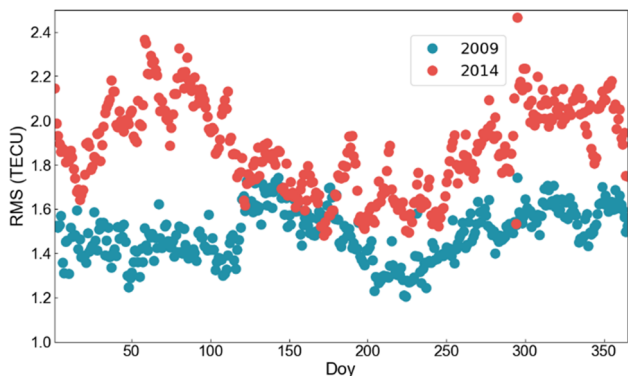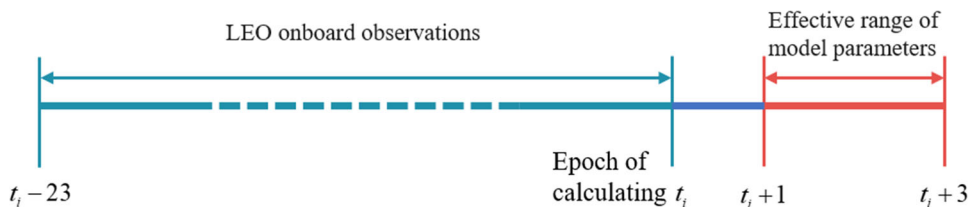

Fig. 10 The daily RMS values of the differences between the topside broadcast models and PodTec observations in 2009 and 2014
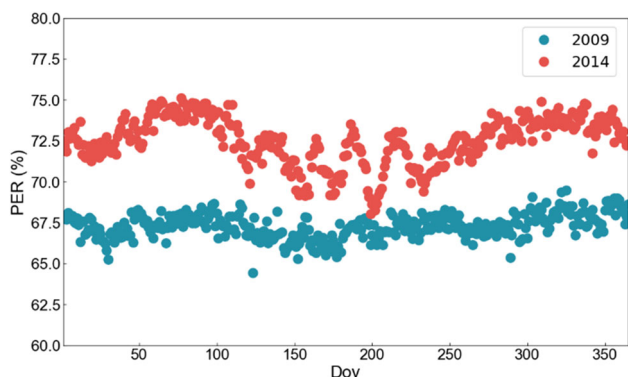

Fig. 11 The daily PER values of the topside broadcast model in 2009 and 2014

Fig. 12 **a**, **b** and **c** represent the variation in the topside ionospheric yearly average TEC, RMS, and PER, respectively, with LT in 2009 and 2014

ionospheric model in 2009 and 2014, and the LT variation of yearly PER in 2009 and 2014 have the similar tendency. The PER value decreases during LT 0:00–3:00 and 15:00–22:00, and increases during 4:00–12:00. The peak appears at LT 13:00 in 2009 and the value is 69.16%. In 2014, the peak appears at LT 12:00 and the value is 74.58%.

The previous sections present the performance of the model at different times. This section demonstrates the performance of the broadcast model in terms of latitudinal behavior. From Table 1, the PodTec cannot provide abundant information in the region beyond 72º as only the Metop-A's inclination is over 72º. During the accuracy evaluation process, the number of reference values available in the region above 72º is limited, resulting in unreliable accuracy evaluation results. Thus, this section focuses on the model's
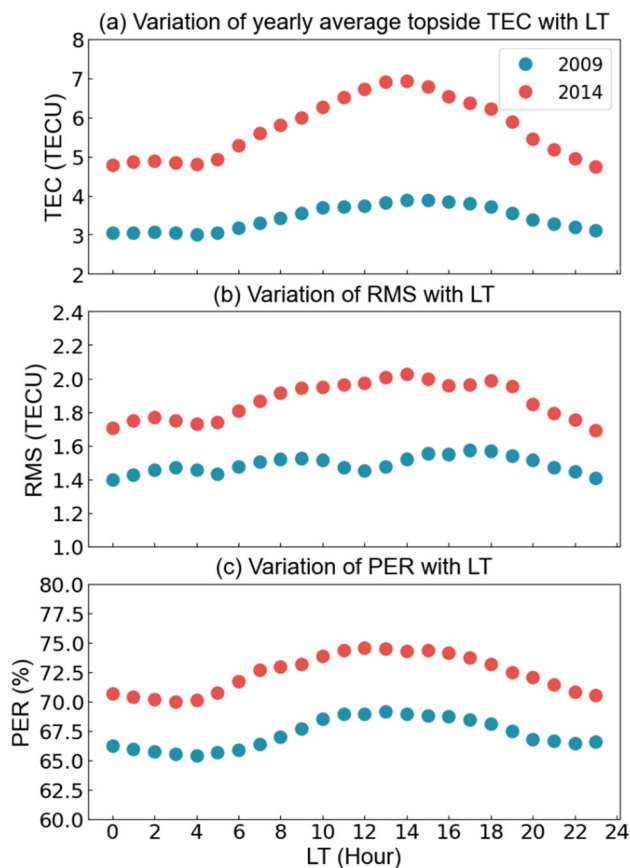
performance in the region within 72º latitude. Figure 13a shows the variation in yearly average topside TEC with latitude in 2009 and 2014. The variation in 2009 and 2014 has the same tendency. The values of the topside TEC in 2009 and 2014 reach the maximum at the equator, and the maximum values are 4.47 and 7.51 TECU. Figure 13b shows the variation in the model's RMS with latitude in 2009 and 2014. The maximum value of RMS, 2.29 TECU, in 2014, also reaches the equator. There is no significant difference in the region between 30º south latitude and 30º north latitude in 2009, and the values are approximately 1.60 TECU. The RMS increases at latitudes higher than 60ºS and 62.5ºN in 2009. In 2014, it increases at latitudes higher than 50ºS and 60ºN. The variation in the model's PER with latitude in 2009
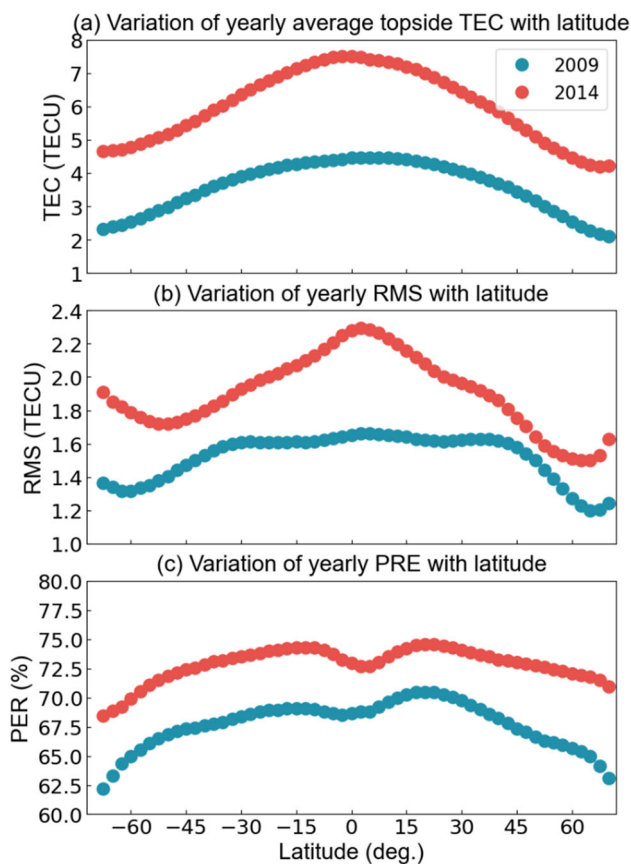
Fig. 13 a, **b** and **c** represent the variation in the topside ionospheric yearly average TEC, RMS, and PER with latitude in 2009 and 2014, respectively

and 2014 is shown in Fig. 13c. In region below 60°, the PER is more than 70% in 2014, and it is more than 60% in 2009.

5 Conclusions and discussion

The LEO global broadcast ionospheric delay correction model is an important component of the LEO-NA service system. Considering that there are no ground station observations from LEO satellites and there are many available LEO onboard observations, the bottom-side broadcast ionospheric delay can be calculated from the topside and GNSS global broadcast ionospheric delay correction model. In this paper, a solution, adopting 2nd order SH function model as topside broadcast ionospheric model, is proposed to facilitate single-frequency LEO-NA ionospheric corrections in the future.

The performance of different order SH models is evaluated in producing a global topside ionospheric model. As the order of the spherical harmonic function increases, the resolution of the global ionospheric TEC gradually increases, and the internal and external accuracy improves. When the order is

increased from 1 to 2, the internal and external accuracy of the model significantly improves. With the values from the 8th order spherical harmonic functions regarded as the reference ionosphere VTEC, the value of RMS is 0.54 TECU, and the correction percentage is 78.51% in the 2nd order SH model. As the order continues to increase, the improvement in modelling accuracy does not show significant changes.

Since significantly less data capacity is desirable for communication, the number of broadcast coefficients for ionospheric model is limited. The maximum information carried by all 81 coefficients of the eighth-order SH model is truncated to the first 9 coefficients. The number of the 2nd order SH model is also 9, the difference between GTIMs obtained from the initial 9 coefficients of the 8th order SH model and the 2nd order SH model is calculated. Compared to the LEO topside ionosphere, the difference can be ignored. Considering the lower data capacity in the navigation message, the ionospheric model's accuracy, and the modelling's computational efficiency, the 2nd order spherical harmonic function model is selected as the topside ionosphere broadcast model. Moreover, the strategy of updating the LEO-NA topside broadcast ionospheric parameters is consistent with BDGIM.

The performances of the topside global broadcast ionospheric delay correction models in 2009 and 2014 are evaluated. The mean RMS values in 2009 and 2014 are 1.49 TECU and 1.88 TECU. The mean values of PER in 2009 and 2014 are 67.30% and 72.49%, respectively. The values of PER and RMS are more stable in 2009 than those in 2014. The yearly PER and LT relationship is similar in 2009 and 2014. The peak appears at LT 13:00 in 2009 and the value is 69.16%. In 2014, the peak appears at LT 12:00 and the value is 74.58%. However, there are some differences in the relationship between RMS and time in 2009 and 2014. In 2009, it reaches the daily maximum value, 1.57 TECU, at LT 18:00. In 2014, the maximum value is 2.03 TECU at 14:00. In addition, the performance of the broadcast model in terms of latitudinal behaviour is analysed. The maximum value of RMS, 2.29 TECU, in 2014, reaches at the equator. However, there is no significant difference in the region between 30° south latitude and 30° north latitude in 2009, and the values are approximately 1.60 TECU. In region below 60°, the PER is more than 70% in 2014, and it is more than 60% in 2009.

From the study of practical LEO-NA and designing LEO-NA constellation, the orbit is between 700–1500 km. Limited by the number of LEO satellites at the same orbital altitude, it is difficult to establish the global ionospheric model and show the performance of the solution at other orbital altitude. This solution considers many issues in actual system construction, including the absence of LEO global station observations, data capacity limitations in the navigation message, and the necessity for accurate ionosphere correction. The broadcast ionospheric solution demonstrates universality, making it

suitable for widespread and effective implementation across LEO navigation systems at different altitudes that require ionospheric delay correction. For low Earth orbit navigation systems with orbital altitudes different from 800 km, the performance of the model exhibits a slightly different accuracy compared to the statistical results presented in the paper. In addition, there are no ground station observations from the LEO, and the bottom ionospheric delay correction performances from the topside and GNSS global broadcast ionospheric delay correction models cannot be evaluated. The next step of our work will focus on mapping topside ionospheric VTEC from multiple LEO satellites at different orbital altitudes to prove this solution. Moreover, we will use ground station observations in building the broadcast ionosphere model from LEO at the appropriate time in the development of the LEO system.

Author contributions YY, FG, CT and MW proposed this study and developed the methodology. KL, XZ, and ET conducted the experiments for data collection and processing. YY and FG wrote the manuscript. CT and MW edited the manuscript. All authors were involved in discussions and provided critical feedback to the manuscript.

Data availability We are very grateful to CONSTELLATION OBSERVING SYSTEM FOR METEOROLOGY IONOSPHERE AND CLIMATE for providing the relevant date of the LEO satellites via https://data.cosmic.ucar.edu/gnss-ro/.

References

Angrisano A, Gaglione S, Gioia C, Massaro M, Robustelli U (2013) Assessment of NeQuick ionospheric model for Galileo single-frequency users. Acta Geophys 61:1457–1476

Abhigna M, Sridhar M, Harsha P, Krishna K, Ratnam D (2021) Broadcast ionospheric delay correction algorithm using reduced order adjusted spherical harmonics function for single-frequency GNSS receivers. Acta Geophys 69(1):335–351

CSNO (2012) BeiDou navigation satellite system signal in space interface control document—open service signal B1I (Version 1.0). China Satellite Navigation Office, Dec 2012.

CSNO (2018) BeiDou navigation satellite system signal in space interface control document—open service signal B3I (Version 1.0). China Satellite Navigation Office, Feb 2018

Chen P, Yao Y, Li Q, Yao W (2017) Modeling the plasmasphere based on LEO satellites onboard GPS measurements. J Geophys Res Space Physics 122(1):1221–1233

Deng Z, Ge W, Yin L, Dai S (2023) Optimization design of two-layer Walker constellation for LEO navigation augmentation using a dynamic multi-objective differential evolutionary algorithm based on elite guidance. GPS Solutions 27(1):26–38

Foelsche U, Kirchengast G (2002) A simple "geometric" mapping function for the hydrostatic delay at radio frequencies and assessment

of its performance. Geophys Res Lett 29:10. https://doi.org/10.1029/2001GL013744

Ge H, Li B et al (2022) LEO enhanced global navigation satellite system (LeGNSS): progress, opportunities, and challenges. Geo Spat Inf Sci 25(1):1–13

Guo F, Yang Y, Ma F, Zhu Y, Liu H, Zhang X (2023) Instantaneous velocity determination and positioning using Doppler shift from a LEO constellation. Satell Navig 4(1):9–21

Hernández-Pajares M, Juan JM, Sanz J, Aragón-Àngel À, García-Rigo A, Salazar D, Escudero M (2011) The ionosphere: effects, GPS modelling and the benefits for space geodetic techniques. J Geodesy 85:887–907

ICD-GPS-200 (1983) Navistar GPS Space Segment/Navigation User Interfaces (Initial release). GPS Joint Program Office, Jan 1983

Jin S, Gao C, Yuan L, Guo P, Calabia A, Ruan H, Luo P (2021) Long-term variations of plasmaspheric total electron content from topside GPS observations on LEO satellites. Remote Sensing 13(4):545–560

Klobuchar JA (1991) Ionospheric effects on GPS. GPS World 4(2):48–51

Kelley, M. C. (2009) The Earth's ionosphere: plasma physics and electrodynamics. Academic press.

Lee HB, Jee G, Kim YH, Shim JS (2013) Characteristics of global plasmaspheric TEC in comparison with the ionosphere simultaneously observed by Jason-1 satellite. J Geophys Res Space Phys 118(2):935–946

Li X, Ma F, Li X, Lv H, Bian L, Jiang Z, Zhang X (2019) LEO constellation-augmented multi-GNSS for rapid PPP convergence. J Geodesy 93:749–764

Li W, Yang Q, Du X et al (2024) LEO augmented precise point positioning using real observations from two CENTISPACE™ experimental satellites. GPS Solutions 28(1):44–56

Liu T, Zhang B, Yuan Y, Zhang X (2020) On the application of the raw-observation-based PPP to global ionosphere VTEC modelling: an advantage demonstration in the multi-frequency and multi-GNSS context. J Geodesy 94:1–20

Ma F, Zhang X, Li X, Cheng J, Guo F, Hu J, Pan L (2020) Hybrid constellation design using a genetic algorithm for a LEO-based navigation augmentation system. GPS Solut 24:1–14

Ma F, Zhang X, Hu J, Li P, Pan L, Yu S, Zhang Z (2022) Frequency design of LEO-based navigation augmentation signals for dual-band ionospheric-free ambiguity resolution. GPS Solut 26(2):53–69

Prieto-Cerdeira R, Orus-Peres R, Breeuwer E, Lucas-Rodriguez R, Falcone M (2014) Performance of the Galileo single-frequency ionospheric correction during in-orbit validation. GPS World 25(6):53–58

Ren X, Zhang X, Xie W, Zhang K, Yuan Y, Li X (2016) Global ionospheric modelling using multi-GNSS: BeiDou, Galileo. GLONASS GPS Sci Rep 6(1):33499

Ren X, Zhang X, Schmidt M, Zhao Z, Chen J, Zhang J, Li X (2020) Performance of GNSS global ionospheric modeling augmented by LEO constellation. Earth Space Sci 7:e2019EA000898. https://doi.org/10.1029/2019EA000898

Ren X, Chen J, Zhang X, Schmidt M, Li X, Zhang J (2020b) Mapping topside ionospheric vertical electron content from multiple LEO satellites at different orbital altitudes. J Geodesy 94:1–17

Schaer S (1999) Mapping and predicting the Earth's ionosphere using the global positioning system. Ph.D. dissertation, University of Bern, Bern.

Wang N (2017) Study on GNSS Differential Code Biases and Global Broadcast Ionospheric Models of GPS, Galileo and BDS. Acta Geod Et Cartogr Sini 46(8):1069–1069

Wang N, Li Z, Yuan Y, Huo X (2021) BeiDou Global Ionospheric delay correction Model (BDGIM): performance analysis during different levels of solar conditions. GPS Solut 25(3):97–109

Yuan Y, Huo X, Zhang B (2017) Research progress of precise models and correction for GNSS ionospheric delay in China over recent years. Acta Geod Et Cartogr Sini 46(10):1364–1378

Yuan Y, Wang N, Li Z, Huo X (2019) The BeiDou global broadcast ionospheric delay correction model (BDGIM) and its preliminary performance evaluation results. Navigation 66(1):55–69

Zhong J, Lei J, Dou X, Yue X (2016) Assessment of vertical TEC mapping functions for space-based GNSS observations. GPS Solut 20:353–362

Zha J, Zhang B, Liu T, Hou P (2021) Ionosphere-weighted undifferenced and uncombined PPP-RTK: theoretical models and experimental results. GPS Solut 25(4):135–146

Zhang B, Hou P, Zha J, Liu T (2022a) PPP–RTK functional models formulated with undifferenced and uncombined GNSS observations. Satell Navig 3(1):3–17

Zhang Q, Liu Z, Hu Z, Zhou J, Zhao Q (2022b) A modified BDS Klobuchar model considering hourly estimated night-time delays. GPS Solut 26(2):49–61